1521-0111/12/8202-310–321
MOLECULAR PHARMACOLOGY
U.S. Government work not protected by U.S. copyright
Mol Pharmacol 82:310–321, 2012

Vol. 82, No. 2
76752/3783672

Telomere and Microtubule Targeting in Treatment-Sensitive and Treatment-Resistant Human Prostate Cancer Cells

Bin Zhang, Silke Suer, Ferenc Livak, Samusi Adediran, Arvind Vemula, Mohammad Afnan Khan, Yi Ning, and Arif Hussain

University of Maryland Greenebaum Cancer Center (B.Z., F.L., S.A., A.V., M.A.K, A.H.) and Department of Pathology (Y.N.), University of Maryland School of Medicine, Baltimore, Maryland; Barbara Ann Karmanos Cancer Center, Wayne State University School of Medicine, Detroit, Michigan (S.S.); and Baltimore Veterans Affairs Medical Center, Baltimore, Maryland (A.H.)

Received November 14, 2011; accepted May 14, 2012

ABSTRACT

Modulating telomere dynamics may be a useful strategy for targeting prostate cancer cells, because they generally have short telomeres. Because a plateau has been reached in the development of taxane-based treatments for prostate cancer, this study was undertaken to evaluate the relative efficacy of targeting telomeres and microtubules in taxane-sensitive, taxane-resistant, androgen-sensitive, and androgen-insensitive prostate cancer cells. Paclitaxel- and docetaxel-resistant DU145 cells were developed and their underlying adaptive responses were evaluated. Telomere dynamics and the effects of targeting telomeres with sodium meta-arsenite (KML001) (an agent undergoing early clinical trials), including combinations with paclitaxel and docetaxel, were evaluated in parental and drug-resistant cells. The studies were extended to androgen-sensitive LNCaP cells and androgen-insensitive LNCaP/C81 cells. Both P-glycoprotein (Pgp)-dependent and non–Pgp-dependent mechanisms of resistance were recruited within the same population of DU145 cells with selection for drug resistance. Wild-type DU145 cells have a small side population (SP) (0.4–1.2%). The SP fraction increased with increasing drug resistance, which was correlated with enhanced expression of Pgp but not breast cancer resistance protein. Telomere dynamics remained unchanged in taxane-resistant cells, which retained sensitivity to KML001. Furthermore, KML001 targeted SP and non-SP fractions, inducing DNA damage signaling in both fractions. KML001 induced telomere erosion, decreased telomerase gene expression, and was highly synergistic with the taxanes in wild-type and drug-resistant DU145 cells. This synergism extended to androgen-sensitive and androgen-insensitive LNCaP cells under basal and androgen-deprived conditions. These studies demonstrate that KML001 plus docetaxel and KML001 plus paclitaxel represent highly synergistic drug combinations that should be explored further in the different disease states of prostate cancer.

Introduction

The microtubular network represents an important target for the treatment of prostate cancer, particularly advanced, castration-resistant disease. Although the microtubule-targeting agent docetaxel has improved overall survival rates for men with metastatic prostate cancer, not all patients respond to it (Petrylak et al., 2004; Tannock et al., 2004; Berthold et al., 2008). Even for men who respond to docetaxel, the treatment is primarily palliative, because most patients experience disease progression within a few months. To improve response rates and response durations, a number of agents have been evaluated in various combinations with docetaxel. To date, however, no docetaxel-based combination regimen has been shown to be superior to single-agent docetaxel treatment for castration-resistant prostate cancer in phase III trials. The overall situation for patients with metastatic, castration-resistant prostate cancer is beginning to change with the approval of several treatments, including

This work was supported by the Department of Defense [Grant PC081047] and the Department of Veterans Affairs (Medical Research Service Merit Review Award to A.H.). S.S. was supported in part by a grant from Komipharm International Co. (Kyongki-Do, South Korea).

B.Z. and S.S. contributed equally to this work.

Article, publication date, and citation information can be found at http://molpharm.aspetjournals.org.

http://dx.doi.org/10.1124/mol.111.076752.

ABBREVIATIONS: KML001, sodium meta-arsenite; ABC, ATP-binding cassette; APL, acute promyelocytic leukemia; AR, androgen receptor; wt, wild-type; ATO, arsenic trioxide; BCRP, breast cancer resistance protein; CI, combination index; DRI, dose reduction index; FACS, fluorescence-activated cell sorting; FAM, fluorescein amidite; FISH, fluorescence in situ hybridization; HBSS, Hanks' balanced salt solution; PBS, phosphate-buffered saline; hTERT, human telomere reverse transcriptase; PE, phycoerythrin; Pgp, P-glycoprotein; PCR, polymerase chain reaction; PNA, peptide nucleic acid; SP, side population; VP, verapamil; MTT, 3-(4,5-dimethylthiazol-2-yl)-2,5-diphenyltetrazolium bromide; Ko143, (3*S*,6*S*,12a*S*)-1,2,3,4,6,7,12,12a-octahydro-9-methoxy-6-(2-methylpropyl)-1,4-dioxopyrazino[1′,2′:1,6]pyrido[3,4-*b*]indole-3-propanoic acid 1,1-dimethylethyl ester; Hoechst 33342, 2′-(4-ethoxyphenyl)-5-(4-methyl-1-piperazinyl)-2′,5′-bi-1*H*-benzimidazole.

sipuleucel-T, cabazitaxel, abiraterone, and denosumab (Kantoff et al., 2010; de Bono et al., 2010, 2011; Fizazi et al., 2011). Despite such progress, most men with metastatic prostate cancer are likely to succumb eventually to their disease.

With respect to taxanes, several mechanisms of inherent or acquired resistance have been implicated in their limited activity in prostate cancer (Greenberger and Sampath, 2006). Included among these resistance mechanisms are altered expression of drug efflux pumps and qualitative changes in the microtubules themselves, which may affect drug-target interactions.

We undertook the present study in an effort to understand more completely some of the adaptive responses of prostate cancer to taxanes and to identify new targets that might be exploited for better therapeutic effects in both drug-sensitive and drug-resistant prostate cancer cells. With DU145 cells as a model of androgen-independent prostate cancer, a series of cell lines with varying levels of resistance to both paclitaxel and docetaxel were developed, to study adaptive responses to taxane selection. Because telomere length maintenance has been implicated in resistance to certain cytotoxic agents, we also investigated telomere dynamics in the aforementioned models (Burger and Harnden, 1998; Ishibashi and Lippard, 1998; Multani et al., 1999; Mo et al., 2003; Deschatrette et al., 2004; Smith et al., 2009). Because prostate cancer cells have short telomeres and may be particularly susceptible to telomere-disrupting agents, we evaluated the role of targeting telomeres in both taxane-sensitive and taxane-resistant prostate cancer cells. These studies were extended to androgen-sensitive LNCaP and androgen-insensitive LNCaP/C81 cells.

In this report, we demonstrate that 1) considerable heterogeneity in resistance mechanisms exists within the paclitaxel- and docetaxel-selected DU145 cell populations, although they share a common phenotype of resistance to taxanes; 2) telomerase activity and telomere lengths are not significantly altered between drug-sensitive and drug-resistant DU145 cells, and they remain sensitive to a telomere-targeting arsenical compound, sodium meta-arsenite (KML001), irrespective of the underlying resistance mechanisms; 3) KML001 can decrease telomerase gene expression, can cause erosion of telomeres, and is synergistic with both paclitaxel and docetaxel in wt and highly taxane-resistant prostate cancer cells; and 4) this synergism extends to androgen-sensitive LNCaP cells and androgen-insensitive LNCaP/C81 cells, under both basal and androgen-deprived conditions. These studies provide a rationale for simultaneously targeting telomeres and microtubules in prostate cancer, including treatment-naive and treatment-resistant (chemotherapy- and castration-resistant) prostate cancer.

Materials and Methods

Cell Lines and Drugs. DU145 human prostate cancer cells were cultured in Dulbecco's modified Eagle's medium/F12 medium (Invitrogen, Carlsbad, CA) supplemented with 5% fetal bovine serum (Gemini, West Sacramento, CA). LNCaP cells (passage numbers of ≤30) were cultured in RPMI 1640 medium supplemented with 10% fetal bovine serum. LNCaP/C81 cells (designated C81 cells) were provided by Dr. Anne Hamburger (University of Maryland Cancer Center, Baltimore, MD). C81 cells were derived from LNCaP cells but had passage numbers of ≥81. The C81 cells were cultured in phenol red-free RPMI 1640 medium supplemented with charcoal-stripped serum (Gemini). Paclitaxel-resistant DU145 cells were derived from parental DU145 cells through incremental exposure of the latter to increasing concentrations of drug. First, wt DU145 cells were exposed to 0.5 nM paclitaxel (IC_{50} dose). Surviving cells were then treated sequentially with increasing doses of paclitaxel over the course of several months to obtain DU145/Pac1, DU145/Pac10, and DU145/Pac200 cells, whose final drug maintenance concentrations were 1, 10, and 200 nM paclitaxel, respectively. Docetaxel-resistant DU145 cells were obtained in a similar manner; those cells were designated DU145/Doc1, DU145/Doc10, and DU145/Doc60, and their final drug maintenance concentrations were 1, 10, and 60 nM docetaxel, respectively. The selected cells were cultured continuously in drug until the time for particular assays.

Paclitaxel (Bedford Laboratories, Bedford, OH) and docetaxel (sanofi-aventis, Bridgewater, NJ) stock solutions were obtained from the University of Maryland Cancer Center Pharmacy. KML001 (Kominox) was provided by Komipharm International Co. (Kyonggi-Do, South Korea); 50 mM drug stock solutions were prepared in PBS, and aliquots were stored at −20°C. The stock solutions were stable for more than 1 year. Working concentrations were freshly prepared.

Growth Inhibition Assays and Drug Combination Studies. The 3-(4,5-dimethylthiazol-2-yl)-2,5-diphenyltetrazolium bromide (MTT) (Sigma-Aldrich, St. Louis, MO) assay was used to assess the antiproliferative effects of various drugs on our panel of cell lines, according to the method described by Mosmann (1983), with minor modifications. Drug combination studies were performed according to the methods described by Chou and colleagues (Chou and Hayball, 1977; Chou and Talalay, 1984; Chou, 2008). Specifically, two-drug combinations were evaluated with the MTT assay over a range of concentrations, by combining the drugs at their fixed IC_{50} ratios at each point tested. From these experiments, the combination index (CI) values at 50, 75, and 90% effective doses and the dose reduction index (DRI) values for each drug in the combination were determined by using the CalcuSyn program developed by Chou and Hayball (1977). According to this method, drugs are synergistic if the CI is <1, additive if the CI is between 1 and 1.2, and antagonistic if the CI is above those values (Chou and Talalay, 1984; Chou, 2008).

Western Blot Analyses. Western blots were performed as described previously, by using NuPAGE 4 to 12% Bis-Tris gels (Invitrogen) to size-fractionate cell lysates (Tang et al., 2006). Primary antibodies to the following proteins were used in the study: Pgp (Santa Cruz Biotechnology Inc., Santa Cruz, CA), BCRP, actin, and β-tubulin (Sigma-Aldrich).

Side Population Assays, Cell Immunostaining, and Cell Sorting. The side population (SP) assay was performed according to the method described by Goodell et al. (1996). Cells were trypsinized, and 0.5×10^6 cells were resuspended in 1 ml of medium containing 2′-(4-ethoxyphenyl)-5-(4-methyl-1-piperazinyl)-2′,5′-bi-1*H*-benzimidazole (Hoechst 33342) (5 μg/ml) alone, Hoechst 33342 plus 50 μM verapamil (PgP inhibitor), or Hoechst 33342 plus 1 μM (3*S*,6*S*,12a*S*)-1,2,3,4,6,7,12,12a-octahydro-9-methoxy-6-(2-methylpropyl)-1,4-dioxopyrazino[1′,2′:1,6]pyrido[3,4-*b*]indole-3-propanoic acid 1,1-dimethylethyl ester (Ko143) (BCRP inhibitor; kindly provided by Dr. Nakanishi Takeo, University of Maryland Cancer Center). The cells were incubated at 37°C for 90 min, centrifuged at 4°C for 5 min, and then resuspended in ice-cold Hanks' balanced salt solution (HBSS) (Invitrogen) containing 2 μg/ml propidium iodide (Invitrogen). The samples were analyzed by using a LSR I flow cytometer (BD Biosciences, San Jose, CA). Excitation of Hoechst 33342 dye with a UV laser was performed at 350 nm, and fluorescence was measured by using a 450/20-nm band-pass filter (Hoechst dye blue) and a 675-nm optical long-pass edge filter (Hoechst dye red). Propidium iodide was excited with a UV laser, and fluorescence was measured with a 675-nm long-pass edge filter.

For immunostaining, trypsinized cells (0.5×10^6) were washed in HBSS with 2% fetal calf serum and 10 mM HEPES (HBSS+) and were stained with allophycocyanin conjugated mouse anti-human CD44 antibody (BD Biosciences Pharmingen, San Diego, CA), phy-

coerythrin (PE)-conjugated anti-Pgp antibody (Millipore, Temecula, CA), PE-conjugated mouse anti-human CD133 antibody (Miltenyi Biotec, Auburn, CA), fluorescein isothiocyanate-conjugated anti-CD49f antibody (BioLegend, San Diego, CA), and their respective controls. The cells were incubated in the dark on ice for 30 min, washed, and analyzed with a FACSCanto II analytical flow cytometer (BD Biosciences). Data were analyzed by using FlowJo software (Tree Star Inc., Ashland, OR).

Drug-resistant prostate cancer cells (20×10^6) were sorted two ways, i.e., with a digital-upgrade FACSVantage Diva cell sorter (BD Biosciences) according to whether they extruded the Hoechst 33342 dye (SP^+ and SP^- fractions) and with a FACSAriaI cell sorter (BD Biosciences) according to whether they expressed Pgp on the cell surface (Pgp^+ and Pgp^- fractions). The gate for SP^+ cells was set on the basis of verapamil inhibition of Hoechst 33342 dye uptake by the treated cells. For sorting according to Pgp status, cells were stained in HBSS+ containing either PE-conjugated anti-Pgp antibody (1:50 dilution) or PE-conjugated isotype-specific antibody (1:50 dilution) and were incubated in the dark on ice for 30 min. After one wash with HBSS, Pgp expression was detected with a 488-nm laser and a 576/26-nm band-pass filter; sorting gates were set with respect to isotype control staining, which served as a baseline.

Telomeric Repeat Amplification Protocol Assays. Telomerase enzyme activity was measured in cell extracts with the telomeric repeat amplification protocol assay, by using a TeloTAGGG telomerase PCR enzyme-linked immunosorbent assay kit (Roche Diagnostics, Mannheim, Germany), according to the manufacturer's instructions, as we reported previously (Burger, 2002). After the addition of stop solution, the mean absorbance of the samples at 450 nm was determined by using a microtiter plate reader (Synergy 2; BioTek, Winooski, VT).

Mean Telomeric Restriction Fragment Length Analyses. Mean telomeric restriction fragment lengths were determined by using a TeloTAGGG telomere length kit (Roche Diagnostics), according to the manufacturer's instructions. Genomic DNA was isolated by using a DNA extraction kit (QIAGEN, Hilden, Germany). Two micrograms of DNA were digested with Hinf1 and Rsa1 for 2 h at 37°C and were loaded onto 0.8% agarose gels. The DNA was transferred to nylon membranes and hybridized to a digoxigenin-labeled telomere probe, and the telomere-related signals were detected on the basis of chemiluminescence, as described previously (Burger et al., 2005).

Real-Time PCR Assays. Total RNA was extracted from cells by using QIAGEN RNeasy Mini kits (QIAGEN) and was purified through DNase digestion, followed by elution with RNase-free water. First-strand cDNA was synthesized by using an iScript Select cDNA synthesis kit (Bio-Rad Laboratories, Hercules, CA). Real-time PCR was performed with a 7900HT Fast Real-Time PCR system with Fast SYBR Green Master Mix (Applied Biosystems, Foster City, CA). Human telomerase reverse transcriptase (hTERT) primers (TIB Molbiol, Adelphia, NJ) were 5′-ATGTCACGGAGACCACGTTT-3′ (sense) and 5′-GGATGAAGCGGAGTCTGGAC-3′ (antisense). Human glyceraldehyde 3-phosphate dehydrogenase primers were 5′-GGTGGTCTCCTCTGACTTCAACA-3′ (sense) and 5′-GTTGCTGTAGCCAAATTCGTTGT-3′ (antisense). The PCR assays were performed in triplicate. The PCR conditions included enzyme activation at 95°C for 20 s, followed by 40 cycles of denaturing at 95°C for 1 s and annealing/extension at 60°C for 20 s. The specificity of the PCRs was verified through melting curve analysis. In the control samples, no cDNA was added in the PCR assays. hTERT gene expression was normalized with respect to glyceraldehyde 3-phosphate dehydrogenase gene expression and was analyzed by using the $\Delta\Delta C_t$ method (Livak and Schmittgen, 2001).

Fluorescence In Situ Hybridization Assays. DU145 cells were cultured to 70% confluence and metaphase cells were prepared through treatment with colcemid, followed by hypotonic treatment and fixation. FISH was performed by using a peptide nucleic acid (PNA) oligomer probe targeting the telomere repetitive sequence (PNA TelC-FAM probe; PNAbio Inc., Thousand Oaks, CA), according to the manufacturer's instructions. Representative metaphase images were acquired by using an Olympus Provis fluorescence microscope (Olympus, Tokyo, Japan) and an Applied Biosystems imaging system.

FISH assays using flow cytometry were performed according to an established protocol (Baerlocher et al., 2006), with minor modifications. Trypsinized cells were divided into four tubes (2×10^5 cells per tube), washed with hybridization buffer, and resuspended in hybridization mixture (77 mM HEPES, 77 mM NaCl, 3.9% bovine serum albumin, and 29% deionized formamide); 500 nM PNA TelC-FAM probe was added to three of the four tubes. The tubes were incubated at room temperature for 10 min and then at 87°C for 15 min, followed by hybridization at room temperature in the dark for 90 min. The cells were washed four times and then resuspended in HBSS+. Flow cytometry was performed with a FACSCanto II cytometer, and the data were analyzed by using FlowJo software. The mean fluorescence intensity for each hybridized sample was calculated after subtraction of background mean fluorescence intensity (sample without probe). The resulting telomere fluorescence values (the horizontal bars in histogram plots) were used to calculate the telomere lengths in the cells, with respect to the known value for the untreated control samples.

Immunofluorescence Assays. Approximately 1.5×10^4 to 2.0×10^4 cells were seeded on eight-well chamber slides overnight. The cells were fixed and permeabilized through immersion in ice-cold methanol/acetone (1:1) three times, for 1 min each time, and were dried for 15 min. The slides were blocked for 2 h at room temperature with 5% bovine serum albumin in PBS, incubated overnight at 4°C with mouse anti-Pgp antibody, rabbit anti-BCRP antibody, or mouse anti-phospho-γ-H2AX antibody (Millipore) at 1:200 dilution, washed with PBS, and incubated for 2 h with fluorescein isothiocyanate-conjugated rabbit anti-mouse or goat anti-rabbit antibody (Sigma-Aldrich) at 1:200 dilution and then for 5 min with 4′,6-diamidino-2-phenylindole (2 mg/ml; Sigma-Aldrich) at 1:5000 dilution. After being washed with PBS, the slides were mounted with Vectashield mounting medium (Vector Laboratories, Burlingame, CA) and were analyzed at 40× magnification with a Leica DM4000 microscope (Leica, Wetzlar, Germany) and 5.0 Openlab software (PerkinElmer Life and Analytical Sciences, Waltham, MA). Quantification of γ-H2AX focus induction was determined by measuring the mean fluorescence intensity of at least 100 nuclei in each chamber.

Results

Paclitaxel- and Docetaxel-Resistant DU145 Prostate Cancer Cells. The IC_{50} values of paclitaxel and docetaxel for DU145 cells and the drug-resistant sublines are shown in Table 1. Exposure to increasing concentrations of a particular taxane (paclitaxel or docetaxel) resulted not only in increasing resistance to the selecting drug but also in cross-resistance to the taxane not used for the original selection (Table 1). It appeared that the DU145 cells were prone to developing higher levels of resistance to docetaxel than to paclitaxel, irrespective of the original taxane used for selection. For instance, DU145/Pac10 and DU145/Pac200 cells were 24- and 140-fold resistant, respectively, to paclitaxel (which was used to select them) but were 100- and 400-fold cross-resistant to docetaxel (Table 1). DU145/Doc10 and DU145/Doc60 cells were 100- and 500-fold resistant, respectively, to their selecting drug (i.e., docetaxel) but were only 24- and 100-fold cross-resistant to paclitaxel.

Both paclitaxel and docetaxel are known substrates of Pgp. This transporter was minimally expressed in wt DU145 cells but was significantly overexpressed in the taxane-resistant cells, particularly with the higher levels of drug selection

TABLE 1

Drug sensitivities, telomere lengths, and telomerase activity of various prostate cancer cell lines

IC_{50} values (mean ± S.D.) were based on three independent experiments.

Cell Lines	Paclitaxel		Docetaxel		KML001 IC_{50}	TA Ratio	Mean TRF Length
	IC_{50}	Fold Resistance	IC_{50}	Fold Resistance			
	μM		μM		μM		*kb*
DU145 wt	0.00250 ± 0.00015	1	0.0005 ± 0.0001	1	4.5 ± 1.0	1.00	2.5
DU145/Pac1	0.006 ± 0.002	2.4	0.001 ± 0.001	2	N.D.	N.D.	N.D.
DU145/Pac10	0.060 ± 0.009	24	0.050 ± 0.017	100	9.3 ± 2.1	0.98	2.0
DU145/Pac200	0.35 ± 0.08	140	0.2 ± 0.1	400	13.3 ± 2.0	1.07	3.0
DU145/Doc1	0.0020 ± 0.0003	1	0.001 ± 0.001	2	N.D.	N.D.	N.D.
DU145/Doc10	0.060 ± 0.007	24	0.050 ± 0.004	100	8.5 ± 4.1	1.07	3.5
DU145/Doc60	0.25 ± 0.05	100	0.250 ± 0.009	500	5.6 ± 2.9	0.96	2.9
LNCaP	0.00025 ± 0.00011	1	0.00020 ± 0.00012	1	3.6 ± 1.4	1.18	2.5
LNCaP/C81	0.0010 ± 0.0002	4	0.00040 ± 0.00023	2	2.3 ± 0.8	1.10	2.7

TA ratio, telomerase activity ratio with respect to DU145 cells; TRF, telomere restriction fragment; N.D., not determined.

(Fig. 1A). The other ATP-binding cassette (ABC) transporter, BCRP, was expressed in both wt and resistant cells, but its levels were not modulated with selection for resistance to the taxanes (Fig. 1A). Flow cytometric analyses revealed that Pgp was expressed on the cell surfaces of significant fractions of the DU145/Pac200 (79 ± 6.5%) and DU145/Doc60 (47 ± 4.9%) cell populations (Fig. 1B). BCRP was essentially undetectable on the surfaces of those cells (Fig. 1B). This finding was confirmed through immunohistochemical analyses, which demonstrated cell surface localization of Pgp in DU145/Pac200 and DU145/Doc60 cells but cytoplasmic localization of BCRP in both wt and taxane-resistant cells (data not shown).

Side Population and Roles of Pgp and BCRP in Taxane-Resistant Cells. The localization of Pgp to the surface of the DU145-derived cells suggested that the transporter is likely to be functional in the cells and to contribute to their drug-resistant phenotype. In contrast, the cytoplasmic localization of BCRP suggested that it is not active in the cells, at least with respect to drug transport functions; this was confirmed in flow cytometric assays using the SP assay method developed by Goodell et al. (1996). The SP fraction is functionally defined on the basis of the extrusion of vital dyes such as Hoechst 33342, because of enhanced expression of ABC transporters (Goodell et al., 1996). The SP fraction can be enriched in stem/progenitor cells and generally represents a very small proportion of the total population; for instance, it represents approximately 0.1% of all nucleated cells in the bone marrow of mice, where it corresponds largely to hematopoietic stem cells.

Parental DU145 cells exhibited a small SP fraction (0.4–1.2%) (Fig. 2A). This fraction increased in the cell lines selected for increasing resistance to docetaxel, being approximately 20% in DU145/Doc10 cells and 60% in DU145/Doc60 cells (Fig. 2A). Pgp-dependent exclusion of the dye was confirmed by treating these cells with verapamil (VP). Although VP is a potent inhibitor of L-type calcium channels, it also inhibits Pgp but not BCRP function. It has been used by investigators to assess Pgp-dependent transport (Tsuruo et al., 1981; Grossi and Biscardi, 2004). VP inhibited extrusion of Hoechst 33342 from DU145/Doc10 and DU145/Doc60 cells, resulting in much greater uptake of the dye by those cells (Fig. 2B). The BCRP-specific inhibitor Ko143 had no effect on Hoechst 33342 uptake (Fig. 2C). Taken together, these data

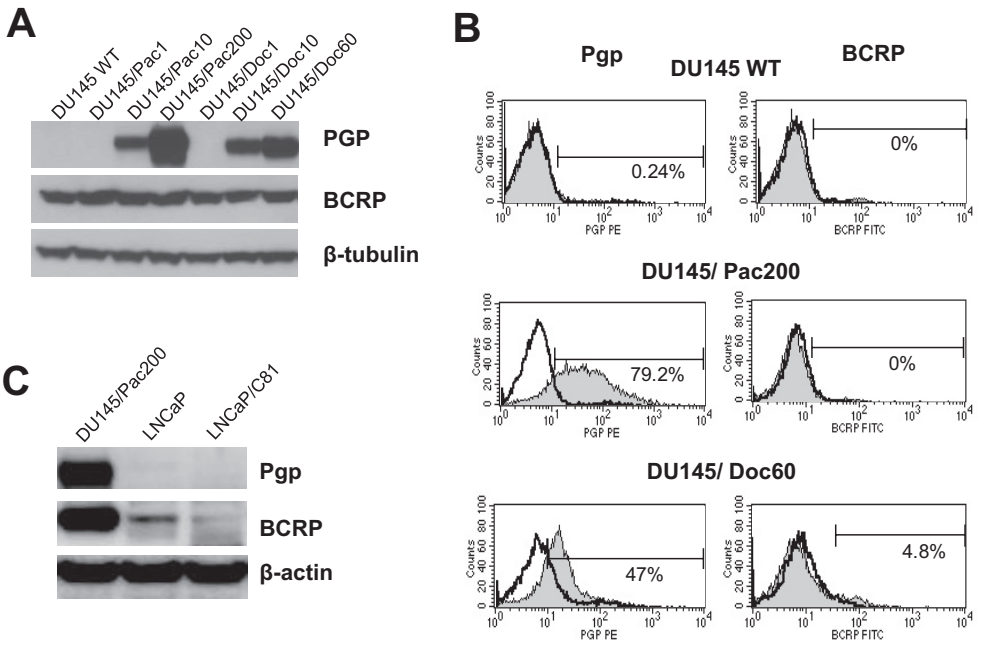

Fig. 1. Pgp and BCRP expression in prostate cancer cells. A, Western blot analysis showing the relative expression of Pgp and BCRP in DU145-derived cell lines. Whole-cell extracts were isolated in modified RIPA buffer, and 50 μg of total protein was loaded in each lane. Western blots are representative of at least three independent experiments. B, flow cytometric analysis showing cell surface expression of Pgp and BCRP in wt and taxane-resistant cells. A total of 0.5×10^6 cells were stained with antibodies, as indicated, for 30 min in the dark. FACS analysis was performed with 10,000 recorded events for each sample. These experiments were repeated three times. Shown are PE- or fluorescein isothiocyanate-stained control cells (white) and PE-Pgp- or fluorescein isothiocyanate-BCRP-positive cells (gray). C, Western blot analysis showing Pgp and BCRP expression in LNCaP and LNCaP/C81 cells; 50 μg of total protein was loaded in each lane.

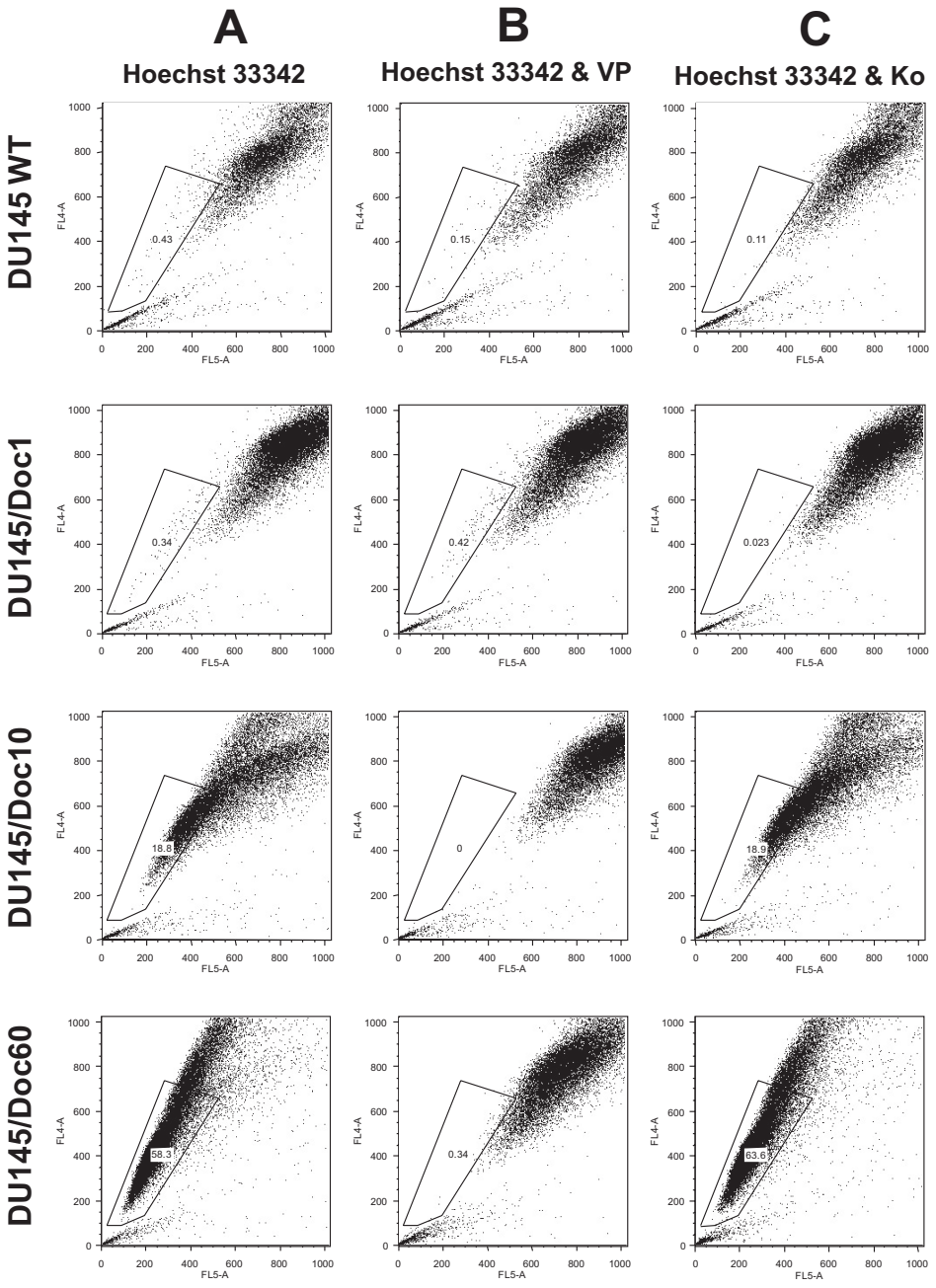

Fig. 2. Flow cytometric analysis. DU145 wt and DU145/Doc cells (0.5×10^6) were resuspended in prewarmed Dulbecco's modified Eagle's medium/F12 medium with Hoechst 33342, in the absence (A) or presence of verapamil (Pgp inhibitor) (B) or Ko143 (Ko) (BCRP inhibitor) (C). The cells were incubated in a 37°C water bath for 90 min. FACS analysis was performed after washing of the cells with ice-cold HBSS. Numbers in the dotted boxes represent the proportions of cells (designated SP) that did not take up Hoechst 33342 because the vital dye was extruded from the cells by Pgp. The data shown are representative of at least four independent experiments.

demonstrate that it is primarily Pgp and not BCRP that is functional in the docetaxel-selected DU145 cells, which is consistent with their respective plasma membrane and cytoplasmic localizations in these cells. Similar results were observed with the DU145/Pac series (data not shown).

Because the SP fraction can contain stem cell-like cells, we evaluated both wt and paclitaxel- and docetaxel-resistant cells for the expression of several stem cell markers, including CD44, CD49f, and CD133, in FACS analyses. Between 28 and 66% of DU145 cells were reported to be $CD44^+$ by different investigators (Patrawala et al., 2006; Stuelten et al., 2010). In our hands, 78 to 88% of wt and taxane-resistant cells were $CD44^+$ (Fig. 3), and almost all of them appeared to express CD49f on their cell surfaces (data not shown). Given the rarity of stem cells, only a small fraction of the aforementioned cells, if any, are likely to be stem cell-like cells in our panel of cell lines. Collins et al. (2005) used another marker, CD133, to identify cancer stem cells in human prostate tumors; 0.1% of the prostate cells were found to be $CD44^+CD133^+$, with a subpopulation with self-renewal properties. Among the DU145 cells, only a small fraction (0.87%) was reported to be $CD133^+$, which would be more consistent with the distribution pattern of a stem cell-like subpopulation (Stuelten et al., 2010). We were not able to identify a $CD133^+$ subpopulation among either wt or taxane-resistant DU145 cells (Fig. 3). Although we might be able eventually to detect some $CD133^+$ cells with optimization of our methods, our data suggest that taxane selection expands the SP population without significantly affecting the distribution patterns of any stem cell-like cells that might exist among the SP cells.

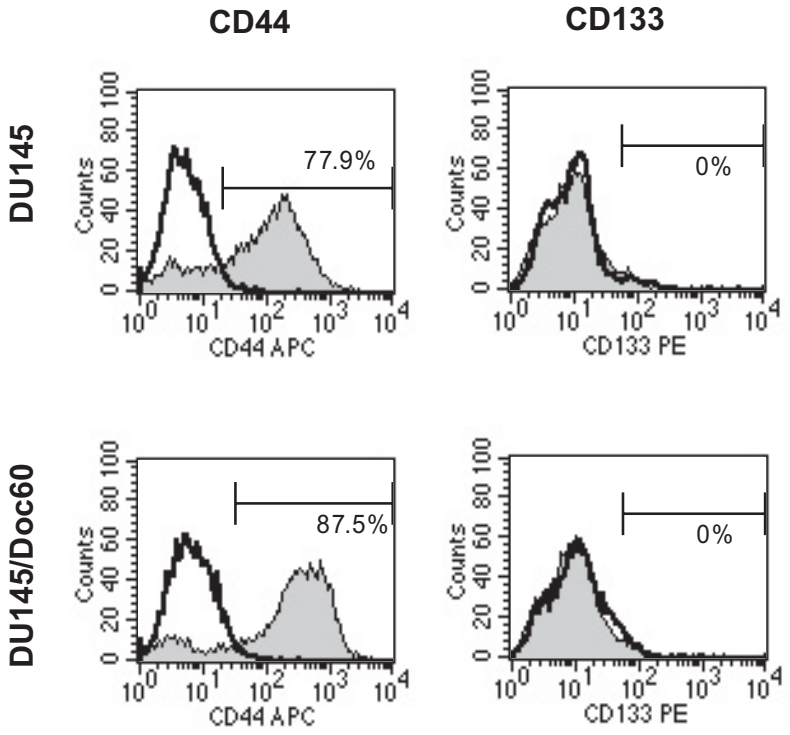

Fig. 3. Immunostaining and flow cytometric analyses. DU145 wt and DU145/Doc60 cells (0.5×10^6) were resuspended in HBSS+ medium and stained with allophycocyanin (APC)-conjugated anti-CD44 antibody, PE-conjugated anti-CD133 antibody, or their respective isotype controls. The cells were incubated on ice for 30 min in the dark. FACS analysis was performed after washing of the cells with ice-cold HBSS+. The numbers reflect the proportions of cells positive for surface CD44 or CD133, compared with isotype control values. The data shown are representative of at least three independent experiments.

Flow Cytometric Analysis of Taxane-Resistant Cells. It is apparent that, in the total DU145/Doc10 and DU145/Doc60 cell populations (as well as among DU145/Pac10 and DU145/Pac200 cells), at least two subpopulations exist, namely, one that is significantly modulated by VP in terms of Hoechst 33342 transport (SP subpopulation) and one that is minimally affected by VP (non-SP subpopulation). To characterize these subpopulations, DU145/Pac200 cells were sorted into SP and non-SP fractions through flow cytometry, to enrich for these fractions. After cell sorting, 91% of total cells (98% of viable cells) in the SP fraction extruded Hoechst 33342 (Fig. 4A, bottom), compared with 65% of cells in the unsorted parental DU145/Pac200 population (Fig. 4A, top). Similarly, the sorted non-SP fraction was enriched primarily for cells that did not extrude Hoechst 33342 (although approximately 15% of the cells in the non-SP fraction could extrude Hoechst 33342, which reflects the limitations of cell sorting on the basis of such functional parameters). Pgp expression in the non-SP fraction was significantly reduced, compared with that in total and SP fractions of DU145/Pac200 cells (Fig. 4B). The non-SP and SP fractions were enriched for non–Pgp-expressing and Pgp-expressing cells, respectively. Although the non-SP fraction exhibited significantly reduced expression of Pgp, the IC_{50} values for paclitaxel in the non-SP and SP fractions were identical, which demonstrated that the two fractions were equally resistant to paclitaxel (Fig. 4C).

We also sorted the parental DU145/Pac200 cells according to cell surface expression of Pgp (Pgp^+ and Pgp^- fractions) (Fig. 4D, bottom). The IC_{50} values for paclitaxel in the Pgp^+ and Pgp^- fractions were identical (Fig. 4E). Taken together, these data demonstrate that, although all DU145/Pac200 cells have the same phenotype of resistance to paclitaxel, there may be different mechanisms of resistance (i.e., Pgp-dependent and non–Pgp-dependent) within the same cell population selected for drug resistance. These Pgp-dependent and non–Pgp-dependent pathways make the cells equally resistant to the selecting drug.

Telomeres, Telomerase Activity, and Telomere Targeting in DU145-Derived Cells. Because the maintenance of telomere lengths is critical for chromosomal integrity in cells, including cancer cells, telomeres and telomerases are emerging as potentially important therapeutic targets (Olaussen et al., 2006). In addition to the well defined property of targeting microtubules, paclitaxel has been shown to cause erosion of telomeres in tumor cell lines (Multani et al., 1999; Mo et al., 2003). Therefore, we wanted to investigate the effects of targeting microtubules and telomeres in the DU145-derived cells. We showed previously that KML001 is a telomere-targeting agent and its cytotoxic effects depend on telomere length; cell lines with short telomeres (such as prostate cancer cells) are more sensitive to KML001 than are those with longer telomeres (Phatak et al., 2008). The effects of paclitaxel and KML001 on parental DU145 cells were assessed with the SP assay (Fig. 5A). In these experiments, approximately 1% of the DU145 cells were within the SP fraction. Paclitaxel at IC_{50} and IC_{100} levels did not decrease the SP fraction of DU145 cells, although the total number of DU145 cells (primarily in the non-SP fraction) was reduced after treatment with paclitaxel; this relative resistance of the SP subpopulation to paclitaxel was likely mediated by an ABC transporter present in SP cells (Fig. 5A). In contrast, KML001 at the IC_{100} significantly reduced the SP fraction of DU145 cells (Fig. 5A).

The IC_{50} values of KML001 for paclitaxel- and docetaxel-resistant DU145 cells were similar, or at most 2- to 3-fold higher, than those for the drug-sensitive wt DU145 cells (Table 1). Because DU145/Pac200 cells had a large SP fraction that could be readily sorted through FACS, we also evaluated the effects of KML001 on the sorted SP and non-SP fractions of DU145/Pac200 cells (Fig. 5, B–D). Figure 5B demonstrates that the SP (primarily Pgp-expressing) and

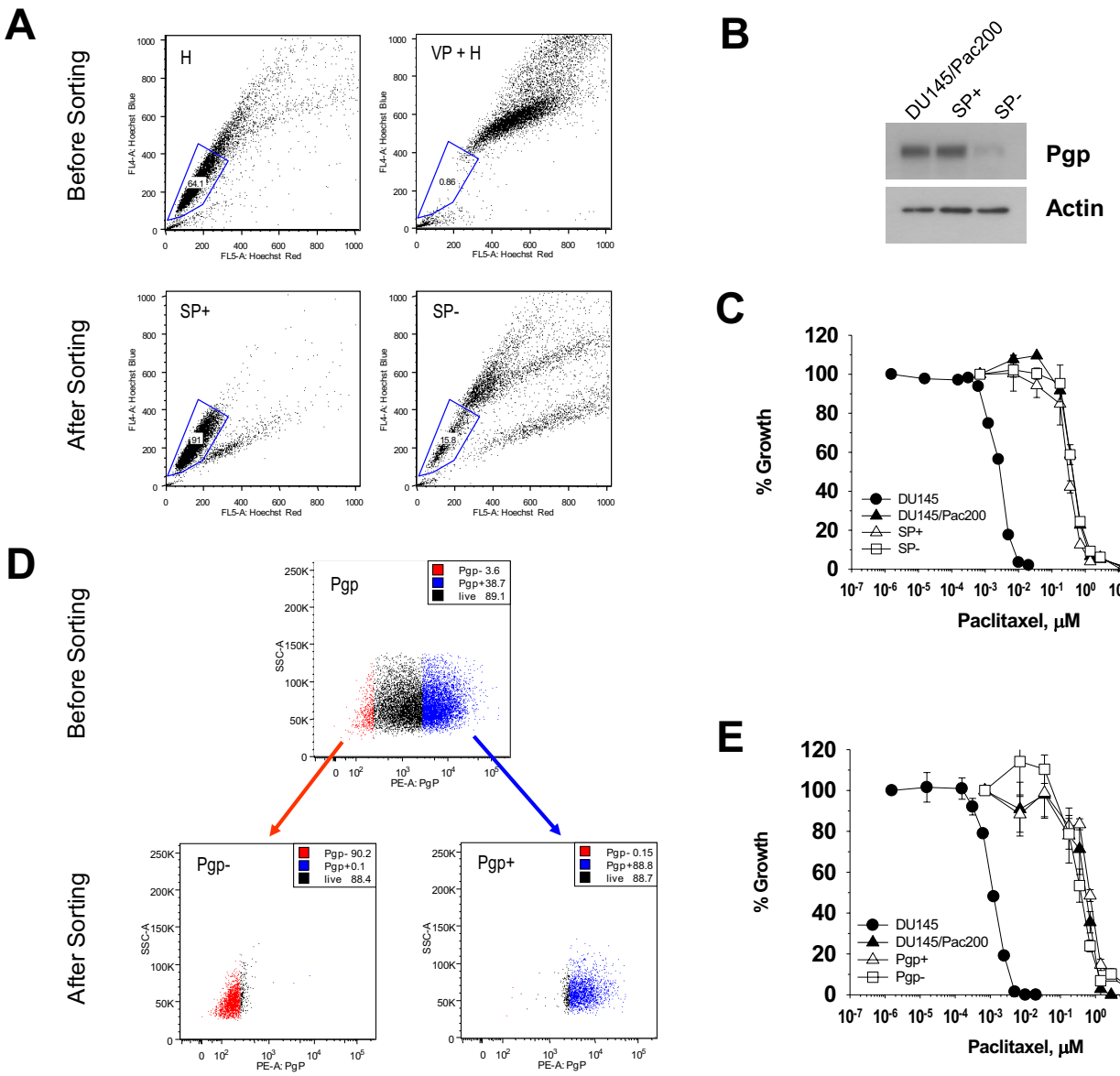

Fig. 4. Analysis of DU145/Pac200 cells sorted through flow cytometry. A, flow cytometric analyses. Top, Hoechst 33342 uptake by DU145/Pac200 cells in the absence or presence of verapamil; bottom, FACS analysis of cells sorted into SP^+ and SP^- groups through gating relative to the VP-suppressible fraction. B, Western blot analysis showing Pgp expression in DU145/Pac200 cells and sorted SP^+ and SP^- cell fractions. One microgram of total protein was loaded in each lane. C, MTT assays with DU145 and DU145/Pac200 cells and SP^+ and SP^- fractions, as described under *Materials and Methods*. D, flow cytometric analyses. Top, cell surface expression of Pgp determined with isotype- or Pgp-specific antibodies; bottom, cells sorted according to whether they expressed cell surface Pgp. E, MTT assays with DU145 and DU145/Pac200 cells and Pgp^+ and Pgp^- fractions.

non-SP (primarily non–Pgp-expressing) cells had similar IC_{50} values for KML001. Uncapping of telomeres can induce DNA damage signaling and responses, including phosphorylation of γ-H2AX at Ser139, which represents an early event of DNA damage signaling (d'Adda di Fagagna et al., 2003; Phatak et al., 2008). KML001 induced phosphorylation of γ-H2AX in wt DU145 and DU145/Pac200 cells, including the SP and non-SP fractions, and more γ-H2AX phosphorylation occurred in the SP fraction than in the non-SP fraction (Fig. 5, C and D). Taken together, the data demonstrate that, unlike paclitaxel, KML001 is a poor Pgp substrate and can target both SP and non-SP cells.

Although modulating telomere dynamics represents a potentially attractive therapeutic strategy, alterations in telomerase activity and telomere lengths have been implicated in resistance to certain cytotoxic agents (Burger and Harnden, 1998; Ishibashi and Lippard, 1998; Deschatrette et al., 2004; Smith et al., 2009). Therefore, we investigated whether any changes in telomerase activity and/or telomere lengths occurred in our panel of taxane-resistant prostate cancer cells. Telomere restriction fragment length analysis showed that, in the prostate cancer cells examined, including paclitaxel- and docetaxel-resistant lines, telomeres were short (2–3 kilobases) and essentially did not change as a consequence of drug selection (Table 1). Telomerase activity also did not change with selection for resistance to either paclitaxel or docetaxel (Table 1). Although DU145 cells could be selected for high levels of resistance to the taxanes, their telomere dynamics were minimally affected, and they remained amenable to telomere targeting.

Importantly, when wt or DU145/Pac200 cells were treated with KML001, paclitaxel, or a combination of the two at their

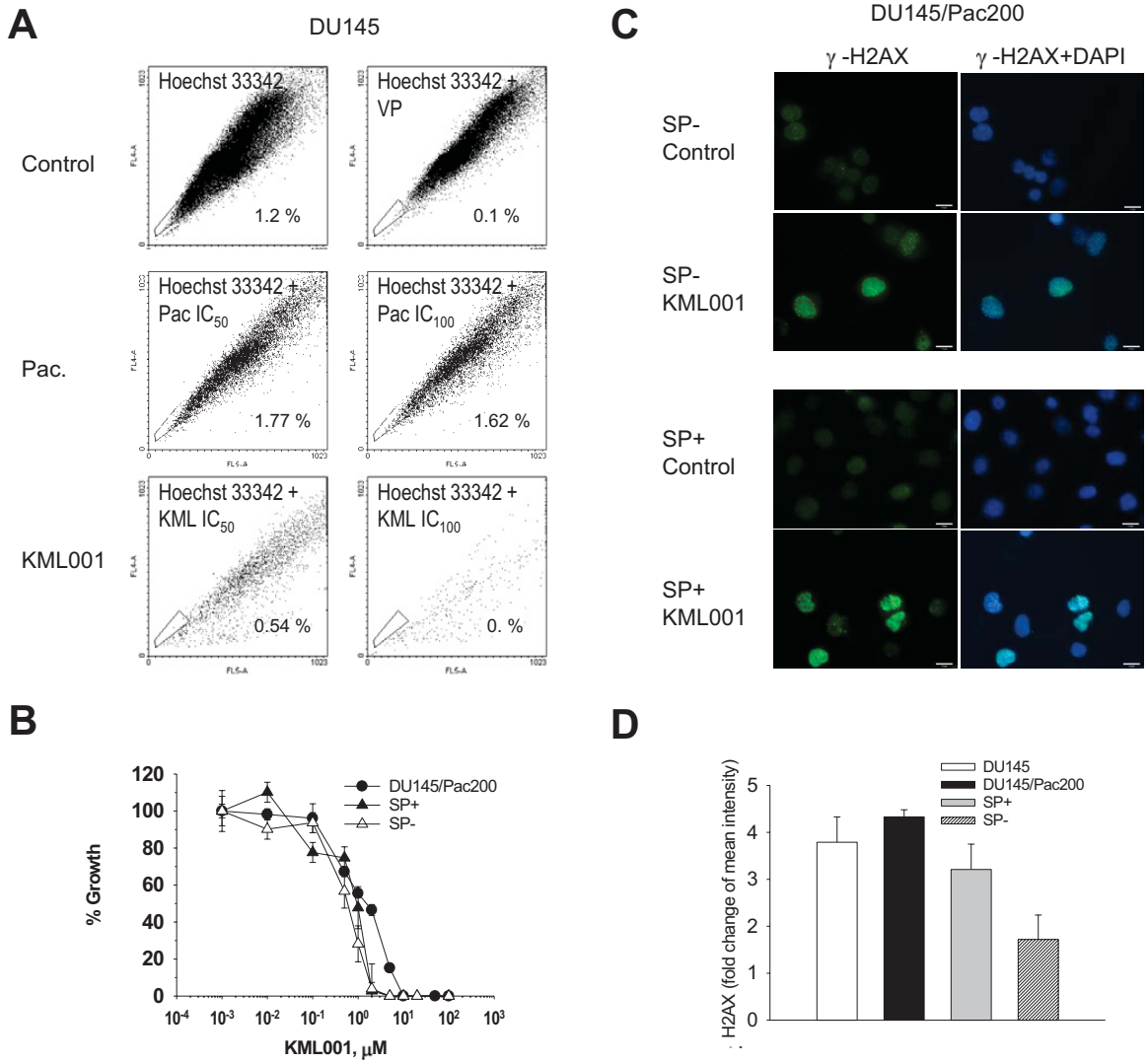

Fig. 5. Effects of KML001 and taxanes on prostate cancer cells. A, SP assay with DU145 cells. Top, cells stained with Hoechst 33342; middle, cells treated with paclitaxel (Pac.) at IC_{50} or IC_{100} for 72 h before Hoechst 33342 staining; bottom, cells treated with KML001 at IC_{50} or IC_{100} for 72 h before Hoechst 33342 staining. B, MTT assays of growth inhibition of DU145/Pac200 cells and SP and non-SP fractions by KML001. C, immunofluorescence analysis of γ-H2AX focus formation (green) in SP^- and SP^+ populations of DU145/Pac200 cells treated with vehicle (control) or KML001 at IC_{100} for 24 h. Shown are representative examples from 10 to 15 independent images. D, mean signal intensity of γ-H2AX foci from at least 100 nuclei per experiment in DU145 and DU145/Pac200 cells and SP^+ and SP^- fractions.

respective IC_{50} values for 3 to 5 days, KML001 or the combination, but not paclitaxel alone, significantly reduced hTERT gene expression (~5-fold) (Fig. 6A and data not shown). We also evaluated the relative integrity of telomeres in response to various treatments, through FACS-coupled FISH analyses. The ability of the FAM-labeled telomere-specific probe to detect telomeres in metaphase spreads of DU145 cells is shown in Fig. 6B. It was apparent that a 72-h incubation with KML001 or KML001 plus paclitaxel at IC_{50} levels led to further telomere shortening, whereas paclitaxel alone had minimal effects (Fig. 6, C and D).

Combining KML001 with paclitaxel or docetaxel at their fixed IC_{50} ratios, according to the method described by Chou and Talalay (1984), to evaluate the dose-effect relationships of the drug combinations demonstrated that the highly resistant DU145/Pac200 cells became less resistant to either taxane in the presence of KML001. In fact, as shown in Fig. 7, the CI values at the 50, 75, and 90% effective doses for KML001 plus paclitaxel or KML001 plus docetaxel in DU145/Pac200 cells were less than 1, which demonstrated synergism between KML001 and the taxanes. CI values also were less than 1 in wt DU145 cells and resistant DU145/Doc60 cells, which indicated synergism in those cell lines (Table 2). Also shown in Table 2 are the calculated DRI values, which represent a measure of the fold reduction in the dose of each drug in a combination needed to yield the same therapeutic effect as observed with the individual drugs alone (Chou, 2008). For both wt and drug-resistant DU145 cells, severalfold dose reductions were predicted for either paclitaxel or docetaxel when combined with KML001.

Studies with Androgen-Sensitive and Androgen-Resistant LNCaP Cells. LNCaP cells have been studied extensively as a cell culture model of androgen-sensitive prostate cancer. It is important to note that, although androgen withdrawal inhibits cell proliferation, such responses of LNCaP cells to androgen deprivation depend on the cell passage number; LNCaP cells at passage numbers below 30 are androgen sensitive, whereas those at passage numbers

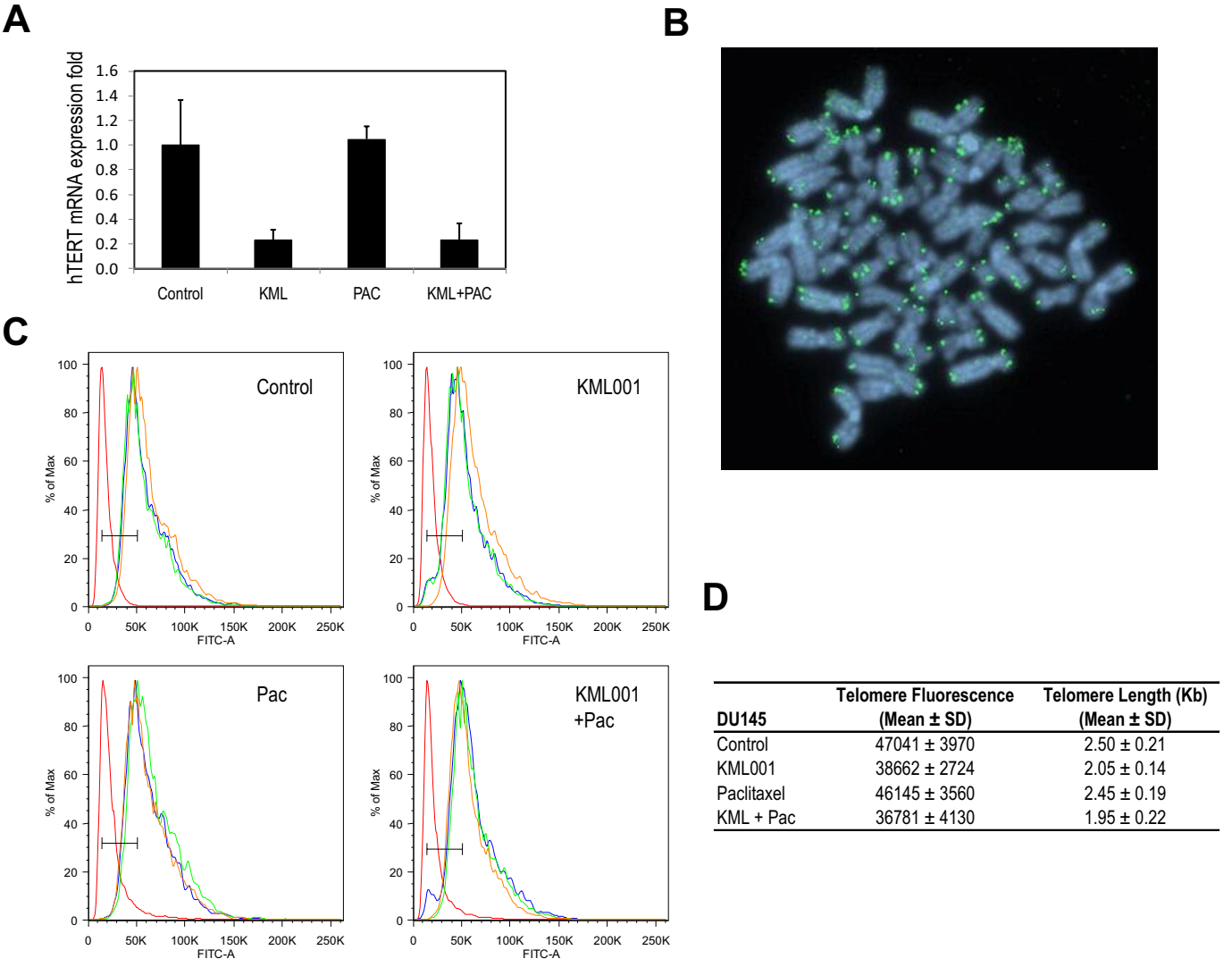

D

DU145	Telomere Fluorescence (Mean ± SD)	Telomere Length (Kb) (Mean ± SD)
Control	47041 ± 3970	2.50 ± 0.21
KML001	38662 ± 2724	2.05 ± 0.14
Paclitaxel	46145 ± 3560	2.45 ± 0.19
KML + Pac	36781 ± 4130	1.95 ± 0.22

Fig. 6. Telomerase gene expression and analysis of telomere lengths. A, real-time PCR analyses. hTERT mRNA expression was evaluated in DU145/Pac200 cells that had been treated for 72 h with KML001, paclitaxel (Pac.), or both drugs, at their IC_{50} levels. The experiments were performed in triplicate. B, metaphase spread for detection of telomeres in DU145 cells with the PNA TelC-FAM probe. C, flow cytometric FISH analyses. Fluorescence histograms (determined in triplicate) are shown for DU145 cells that were treated with KML001, paclitaxel, or KML001 plus paclitaxel, at their IC_{50} levels, for 72 h and then hybridized in situ with the PNA TelC-FAM probe. D, telomere length results. The telomere length for each sample was calculated from the fluorescence histograms after subtraction of the background mean fluorescence intensity (no probe) from the mean fluorescence intensity value obtained through hybridization with the PNA TelC-FAM probe.

above 81 (designated C81) maintain cell proliferation despite androgen withdrawal (Lin et al., 1998). Both LNCaP and C81 cells had small SP fractions (approximately 0.6 and 0.2%, respectively) and did not appear to express Pgp or BCRP to any significant extent (Fig. 1C). The IC_{50} values for paclitaxel, docetaxel, and KML001 in LNCaP and C81 cells are listed in Table 1. Consistent with previous observations that androgen resistance could lead to relative chemoresistance, the C81 cells were 2- and 4-fold more resistant to docetaxel and paclitaxel, respectively, compared with LNCaP cells, but were equally sensitive to KML001 (Table 1). Both cell lines had short telomeres, with essentially identical telomerase activities (Table 1). For both LNCaP and C81 cells, the CI values for the KML001/paclitaxel and KML001/docetaxel combinations were below 1 (Table 2). These findings demonstrated that KML001 was synergistic with both taxanes in both LNCaP and C81 cells. However, the calculated DRI values suggested that LNCaP cells were more sensitive to the taxanes when they were combined with KML001, compared with C81 cells (Table 2).

Although at present we do not know the specific molecular pathways that contribute to the relatively lower DRI values for taxanes in C81 cells, studies regarding the mechanisms of arsenical compound and taxane actions provided important insights that may explain some of the differences in the sensitivities of LNCaP and C81 cells to the KML001/taxane combinations. Two studies identified additional effects of taxanes specifically in prostate cancer (Zhu et al., 2010; Darshan et al., 2011). In particular, those studies showed that microtubules play an integral role in the translocation of the androgen receptor (AR) from the cytoplasm to the nucleus (where it is active) and that disruption of microtubules by taxanes can impair AR activity in prostate cancer. Because LNCaP cells are more responsive/sensitive to the androgen-AR axis than are C81 cells (Lin et al., 1998), this effect of taxanes on AR activity is likely to have a greater impact on

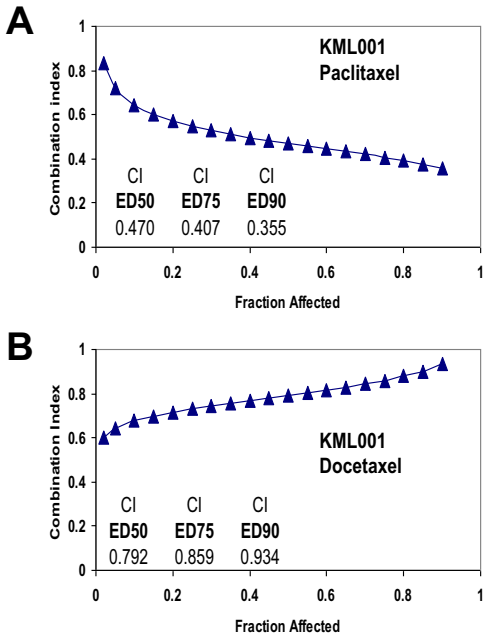

Fig. 7. CI values for DU145/Pac200 cells as a function of cell fraction affected. Top, KML001 plus paclitaxel; bottom, KML001 plus docetaxel. Four thousand cells per well were plated in 96-well plates. After overnight incubation, serial dilutions of single drugs or two-drug combinations at their fixed IC_{50} ratios were added to each well and incubated for 5 days. MTT assays were performed and CI values were determined by using CalcuSyn software.

LNCaP cells. Furthermore, because arsenical compounds can disrupt microtubule dynamics (Li and Broome, 1999; Ling et al., 2002; Cai et al., 2003), KML001 in combination with a taxane is likely to have a greater inhibitory effect in androgen-sensitive prostate cancer cells. Another intriguing action attributed to paclitaxel in prostate cancer cells is that it can enhance the interaction between ARs and FOXO1, which inhibits AR function (Gan et al., 2009). These mechanisms of taxane action are consistent with our observations regarding the prominent synergy between KML001 and taxanes in LNCaP cells; this combination was also active in C81 cells, but to a lesser extent (Table 2).

Discussion

One of the salient features of many cancers, particularly solid tumors, is their significant heterogeneity at the genetic and/or phenotypic levels, which likely contributes to the variable clinical course and outcomes with treatment among patients with seemingly similar tumor types. Furthermore, it is becoming apparent that a small population of cells with stem cell-like properties (i.e., cancer stem cells) exist within many tumors and can give rise to all of the cells in the original tumor (Reya et al., 2001; Visvader and Lindeman, 2008). Such cancer stem cells might contribute to some of the tumor heterogeneity observed clinically.

The observed heterogeneity of clinical tumors is less apparent in established, long-term, cancer cell lines, although cancer cells in culture can demonstrate pleiotropic responses to selective pressure. With respect to taxanes, overexpression of drug efflux pumps and mutations in β-tubulin have been implicated as mechanisms that enable cancer cells to adapt to and survive taxane inhibition (Greenberger and Sampath, 2006). Our panel of DU145 cells up-regulated Pgp in response to selection with both paclitaxel and docetaxel. Figure 1B reveals that the expression of Pgp at the cell surface varied among the different resistant cells that constituted particular paclitaxel- or docetaxel-selected populations. Figure 1B also suggests that 20 to 50% of the cells that constituted the DU145/Pac200 or DU145/Doc60 populations had minimal cell surface expression of Pgp. Studies evaluating Pgp transport function in the resistant cells showed that only a fraction of DU145/Doc10 or DU145/Doc60 cells actually transported Hoechst 33342 (Fig. 2), which is consistent with the proportion of Pgp-expressing, taxane-resistant cells present in these populations.

Importantly, when the paclitaxel-resistant cells were sorted into SP (positive Hoechst 33342 transport) and non-SP (minimal/absent Hoechst 33342 transport) fractions or into cell surface Pgp-positive or cell surface Pgp-negative fractions, the sorted fractions were equally resistant to paclitaxel (Fig. 4). Therefore, both Pgp-dependent and non–Pgp-dependent mechanisms of resistance may be associated with

TABLE 2
Combination index and dose reduction index values for KML001/taxane combinations

Cell Lines and Fraction Affected	KML001 Plus Paclitaxel			KML001 Plus Docetaxel		
	CI	DRI for KML001	DRI for Paclitaxel	CI	DRI for KML001	DRI for Docetaxel
DU145						
0.50	0.835	2.328	2.466	0.805	1.375	12.791
0.75	0.681	2.432	3.699	0.922	1.186	12.732
0.90	0.574	2.541	5.550	1.056	1.023	12.673
DU145/Pac200						
0.50	0.470	6.529	3.156	0.792	1.514	7.637
0.75	0.407	6.674	3.892	0.859	1.370	7.736
0.90	0.355	6.821	4.800	0.934	1.240	7.837
DU145/Doc60						
0.50	1.106	0.985	11.008	0.954	1.116	17.219
0.75	0.877	1.303	9.148	0.766	1.389	21.722
0.90	0.711	1.724	7.602	0.615	1.728	27.403
LNCaP						
0.50	0.559	1.944	22.549	0.341	3.184	37.737
0.75	0.684	1.561	23.199	0.337	3.214	38.352
0.90	0.839	1.255	23.868	0.334	3.243	38.976
LNCaP/C81						
0.50	1.640	2.574	0.799	0.403	7.329	3.745
0.75	0.790	3.242	2.079	0.603	3.966	2.846
0.90	0.430	4.084	5.407	0.928	2.146	2.163

DU145 cells exposed to taxanes. Individual cells may use one or more than one mechanism of resistance. Such plasticity in response to taxane selection within the same DU145 cell population would not have been apparent if only total cell lysates had been analyzed in Western blot analyses (e.g., Fig. 1A). Stem cell-like cells have been identified in long-term cancer cell line cultures, including DU145 cells, which have a small SP fraction (Figs. 2A and 4A) (Stuelten et al., 2010). Whether these stem cell-like cells contribute to the pleiotropic response to taxane selection in DU145 cells is presently not clear. However, it is apparent from these studies that strategies that address only Pgp-based resistance are unlikely to be successful in improving on the current, taxane-based treatments for prostate cancer. Approaches that enhance the effects of taxanes and possibly also address Pgp-related and non–Pgp-related resistance and stem cell-like cell subpopulations need to be developed.

We showed previously that the telomere-targeting agent KML001 is particularly active in cancer cell lines that have short telomeres and is less active in cell lines with longer telomeres (Phatak et al., 2008). Prostate cancer cell lines in general have relatively short telomeres and maintain endogenous telomerase activity; therefore, they are potential targets for telomere-targeting agents (Phatak et al., 2008). It is important to note, however, that the development of drug resistance can result in changes in telomere dynamics (including lengthening or shortening of telomeres and changes in telomerase activity), which appear to depend on the cell type and the specific agents to which cells acquire resistance (Burger and Harnden, 1998; Ishibashi and Lippard, 1998; Deschatrette et al., 2004; Smith et al., 2009). Our panel of drug-resistant DU145 cells continued to maintain short telomeres regardless of the taxane (paclitaxel or docetaxel) used for selection or the levels of resistance acquired by the drug-selected cells (Table 1). Total telomerase activity levels did not appear to be altered between wt and taxane-resistant cells (Table 1), although levels were up to 2-fold higher in the SP fraction, compared with the non-SP fraction, of the highly resistant DU145/Pac200 cells (data not shown). Taken together, these data suggest that targeting of telomeres, particularly with an agent that is a poor Pgp substrate, should be effective against both Pgp-expressing and non–Pgp-expressing, taxane-resistant, prostate cancer cells. Consistent with these observations, KML001 retained significant activity in the taxane-resistant cells, targeting both the SP and non-SP fractions (Fig. 5, B–D).

Although telomere lengths and telomerase activity were not affected by drug selection, KML001 or KML001 in combination with paclitaxel could significantly reduce hTERT gene expression and cause erosion of telomeres (Fig. 6). Drug combination studies revealed that KML001 was synergistic with paclitaxel and docetaxel in both taxane-resistant and wt DU145 cells (Fig. 7 and Table 2). Such synergism also was observed in the androgen-sensitive LNCaP cells and in the androgen-insensitive LNCaP/C81 cells grown in phenol red-free medium supplemented with charcoal-stripped serum (i.e., androgen-deprived conditions) (Table 2).

Table 2 also lists the calculated DRI values for KML001, paclitaxel, and docetaxel in the combination regimens, with the various cell lines. It was apparent from these studies that sensitivity to the taxanes (particularly docetaxel) was significantly enhanced when they were combined with KML001. For instance, the DRI values for docetaxel were 13 in wt DU145 cells and 38 in wt androgen-sensitive LNCaP cells (Table 2), which suggests that 13- to 38-fold less docetaxel could be used in combination with KML001 to produce the same treatment effect as that seen when docetaxel is used alone. Although significant synergism between KML001 and paclitaxel and between KML001 and docetaxel also was noted in DU145/Pac200 and DU145/Doc60 cells, it would be more difficult to eradicate effectively all of the highly taxane-resistant cancer cells with the combination regimens, despite enhanced drug sensitivities, because of the high basal levels of resistance and the limits imposed by the actual drug levels that can be achieved safely in clinical settings. The KML001/taxane combinations are likely to be particularly useful in wt, nonselected, chemotherapy-naive, prostate cancer cells, because of their significantly lower basal IC_{50} values for the taxanes. On the basis of the calculated DRI values, these drug combinations also are likely to be more effective in androgen-sensitive than in androgen-insensitive prostate cancer cells.

KML001 is an orally bioavailable, trivalent, arsenical compound. A paradigm for using arsenical compounds in clinical practice exists for another trivalent arsenical compound, i.e., arsenic trioxide (ATO), which was approved for use for patients with acute promyelocytic leukemia (APL) who experience relapse after initial treatments (Soignet et al., 1998, 2001). ATO is also being used as part of consolidation therapy for the initial treatment of APL (Powell et al., 2010). A recent study pilot-tested the use of ATO as monotherapy for patients with newly diagnosed APL (Ghavamzadeh et al., 2011). Both apoptotic and cytodifferentiative effects have been attributed to ATO, depending on the cellular context, with IC_{50} values for various human cancer cell lines being in the micromolar range (Ajana et al., 2009; Han et al., 2010). Pharmacokinetic studies revealed that such plasma concentrations could be achieved among patients treated with ATO at the doses recommended for APL therapy (Shen et al., 2001; Fox et al., 2008). The paradigm established with ATO suggests that KML001 also may have a role in appropriately defined clinical settings. A phase I pharmacokinetic/pharmacodynamic study evaluating the use of escalating doses of KML001 with fixed-dose cisplatin treatment for solid tumors is currently ongoing in the United States (http://clinicaltrials.gov/ct2/show/NCT01110226).

KML001, like ATO, targets telomeres but may modulate other cellular functions by generating reactive oxygen species or binding to sulfhydryl groups in proteins (Mei et al., 2002; Miller et al., 2002). Regardless of its specific modes of action, it is apparent that KML001/taxane combinations produce significant synergistic antiproliferative effects in several different types of prostate cancer cell lines, which may represent various states of the disease, including androgen-sensitive, androgen-insensitive, taxane-sensitive, and taxane-resistant prostate cancers. Although our results need to be extended to in vivo models in future studies, they raise the intriguing possibility that targeting telomeres with an arsenical compound and targeting microtubules with a taxane may be a useful approach to improving outcomes in prostate cancer, which warrants further evaluation.

Acknowledgments

We dedicate this study to the memory of our dear friend and colleague Dr. Angelika Burger, who was the inspiration behind this

work. Dr. Burger devoted her life to the study of cancer. Tragically, she passed away in May 2011. Dr. Burger's wisdom, courage, grace, and dedication to scientific excellence will be cherished.

Authorship Contributions

Participated in research design: Zhang, Suer, Ning, and Hussain.

Conducted experiments: Zhang, Suer, Livak, Adediran, Vemula, Khan, and Ning.

Contributed new reagents or analytic tools: Livak.

Performed data analysis: Zhang, Suer, Livak, Khan, Ning, and Hussain.

Wrote or contributed to the writing of the manuscript: Zhang, Suer, Livak, and Hussain.

References

Ajana I, Astier A, and Gibaud S (2009) Arsthinol nanosuspensions: pharmacokinetics and anti-leukaemic activity on NB4 promyelocytic leukaemia cells. *J Pharm Pharmacol* **61:**1295–1301.

Baerlocher GM, Vulto I, de Jong G, and Lansdorp PM (2006) Flow cytometry and FISH to measure the average length of telomeres (flow FISH). *Nat Protoc* **1:**2365–2376.

Berthold DR, Pond GR, Soban F, de Wit R, Eisenberger M, and Tannock IF (2008) Docetaxel plus prednisone or mitoxantrone plus prednisone for advanced prostate cancer: updated survival in the TAX 327 study. *J Clin Oncol* **26:**242–245.

Burger AM (2002) Standard TRAP assay, in *Telomeres and Telomerase: Methods in Molecular Biology* (Double JA and Thompson MJ eds) pp 109–124, Humana Press, Totowa, NJ.

Burger AM, Dai F, Schultes CM, Reszka AP, Moore MJ, Double JA, and Neidle S (2005) The G-quadruplex-interactive molecule BRACO-19 inhibits tumor growth, consistent with telomere targeting and interference with telomerase function. *Cancer Res* **65:**1489–1496.

Burger AM and Harnden P (1998) Telomerase in germ cell tumours: inhibition of telomerase activity after cisplatin-based therapy, in *Germ Cell Tumours IV* (Jones I, Appelyard I, Harnden P, and Joffe JK eds) pp 73–80, John Libbey & Co., London.

Cai X, Yu Y, Huang Y, Zhang L, Jia PM, Zhao Q, Chen Z, Tong JH, Dai W, and Chen GQ (2003) Arsenic trioxide-induced mitotic arrest and apoptosis in acute promyelocytic leukemia cells. *Leukemia* **17:**1333–1337.

Chou TC (2008) Preclinical versus clinical drug combination studies. *Leuk Lymphoma* **49:**2059–2080.

Chou TC and Hayball MP (1977) *CalcuSyn for Windows: Multiple-Drug Dose-Effect Analyzer and Manual*, Biosoft, Cambridge, UK.

Chou TC and Talalay P (1984) Quantitative analysis of dose-effect relationships: the combined effects of multiple drugs or enzyme inhibitors. *Adv Enzyme Regul* **22:**27–55.

Collins AT, Berry PA, Hyde C, Stower MJ, and Maitland NJ (2005) Prospective identification of tumorigenic prostate cancer stem cells. *Cancer Res* **65:**10946–10951.

d'Adda di Fagagna F, Reaper PM, Clay-Farrace L, Fiegler H, Carr P, Von Zglinicki T, Saretzki G, Carter NP, and Jackson SP (2003) A DNA damage checkpoint response in telomere-initiated senescence. *Nature* **426:**194–198.

Darshan MS, Loftus MS, Thadani-Mulero M, Levy BP, Escuin D, Zhou XK, Gjyrezi A, Chanel-Vos C, Shen R, Tagawa ST, et al. (2011) Taxane-induced blockade to nuclear accumulation of the androgen receptor predicts clinical responses in metastatic prostate cancer. *Cancer Res* **71:**6019–6029.

de Bono JS, Logothetis CJ, Molina A, Fizazi K, North S, Chu L, Chi KN, Jones RJ, Goodman OB Jr, Saad F, et al. (2011) Abiraterone and increased survival in metastatic prostate cancer. *N Engl J Med* **364:**1995–2005.

de Bono JS, Oudard S, Ozguroglu M, Hansen S, Machiels JP, Kocak I, Gravis G, Bodrogi I, Mackenzie MJ, Shen L, et al. (2010) Prednisone plus cabazitaxel or mitoxantrone for metastatic castration-resistant prostate cancer progressing after docetaxel treatment: a randomised open-label trial. *Lancet* **376:**1147–1154.

Deschatrette J, Ng KH, Gouthière L, Maigné J, Guerroui S, and Wolfrom C (2004) Telomere dynamics determine episodes of anticancer drug resistance in rat hepatoma cells. *Anticancer Drugs* **15:**671–678.

Fizazi K, Carducci M, Smith M, Damião R, Brown J, Karsh L, Milecki P, Shore N, Rader M, Wang H, et al. (2011) Denosumab versus zoledronic acid for treatment of bone metastases in men with castration-resistant prostate cancer: a randomised, double-blind study. *Lancet* **377:**813–822.

Fox E, Razzouk BI, Widemann BC, Xiao S, O'Brien M, Goodspeed W, Reaman GH, Blaney SM, Murgo AJ, Balis FM, et al. (2008) Phase 1 trial and pharmacokinetic study of arsenic trioxide in children and adolescents with refractory or relapsed acute leukemia, including acute promyelocytic leukemia or lymphoma. *Blood* **111:**566–573.

Gan L, Chen S, Wang Y, Watahiki A, Bohrer L, Sun Z, Wang Y, and Huang H (2009) Inhibition of the androgen receptor as a novel mechanism of Taxol chemotherapy in prostate cancer. *Cancer Res* **69:**8386–8394.

Ghavamzadeh A, Alimoghaddam K, Rostami S, Ghaffari SH, Jahani M, Iravani M, Mousavi SA, Bahar B, and Jalili M (2011) Phase II study of single-agent arsenic trioxide for the front-line therapy of acute promyelocytic leukemia. *J Clin Oncol* **29:**2753–2757.

Goodell MA, Brose K, Paradis G, Conner AS, and Mulligan RC (1996) Isolation and functional properties of murine hematopoietic stem cells that are replicating in vivo. *J Exp Med* **183:**1797–1806.

Greenberger LM and Sampath D (2006) Resistance to taxanes, in *Cancer Drug Resistance* (Teicher BA ed) pp 329–358, Humana Press, Totowa, NJ.

Grossi A and Biscardi M (2004) Reversal of MDR by verapamil analogues. *Hematology* **9:**47–56.

Han YH, Moon HJ, You BR, Kim SZ, Kim SH, and Park WH (2010) Effects of arsenic trioxide on cell death, reactive oxygen species and glutathione levels in different cell types. *Int J Mol Med* **25:**121–128.

Ishibashi T and Lippard SJ (1998) Telomere loss in cells treated with cisplatin. *Proc Natl Acad Sci USA* **95:**4219–4223.

Kantoff PW, Higano CS, Shore ND, Berger ER, Small EJ, Penson DF, Redfern CH, Ferrari AC, Dreicer R, Sims RB, et al. (2010) Sipuleucel-Timmunotherapy for castration-resistant prostate cancer. *N Engl J Med* **363:**411–422.

Li YM and Broome JD (1999) Arsenic targets tubulins to induce apoptosis in myeloid leukemia cells. *Cancer Res* **59:**776–780.

Lin MF, Meng TC, Rao PS, Chang C, Schonthal AH, and Lin FF (1998) Expression of human prostatic acid phosphatase correlates with androgen-stimulated cell proliferation in prostate cancer cell lines. *J Biol Chem* **273:**5939–5947.

Ling YH, Jiang JD, Holland JF, and Perez-Soler R (2002) Arsenic trioxide produces polymerization of microtubules and mitotic arrest before apoptosis in human tumor cell lines. *Mol Pharmacol* **62:**529–538.

Livak KJ and Schmittgen TD (2001) Analysis of relative gene expression data using real-time quantitative PCR and the $2^{-\Delta\Delta C_T}$ method. *Methods* **25:**402–408.

Mei N, Kunugita N, Hirano T, and Kasai H (2002) Acute arsenite-induced 8-hydroxyguanine is associated with inhibition of repair activity in cultured human cells. *Biochem Biophys Res Commun* **297:**924–930.

Miller WH Jr, Schipper HM, Lee JS, Singer J, and Waxman S (2002) Mechanisms of action of arsenic trioxide. *Cancer Res* **62:**3893–3903.

Mo Y, Gan Y, Song S, Johnston J, Xiao X, Wientjes MG, and Au JL (2003) Simultaneous targeting of telomeres and telomerase as a cancer therapeutic approach. *Cancer Res* **63:**579–585.

Mosmann T (1983) Rapid colorimetric assay for cellular growth and survival: application to proliferation and cytotoxicity assays. *J Immunol Methods* **65:**55–63.

Multani AS, Li C, Ozen M, Imam AS, Wallace S, and Pathak S (1999) Cell-killing by paclitaxel in a metastatic murine melanoma cell line is mediated by extensive telomere erosion with no decrease in telomerase activity. *Oncol Rep* **6:**39–44.

Olaussen KA, Dubrana K, Domont J, Spano JP, Sabatier L, and Soria JC (2006) Telomeres and telomerase as targets for anticancer drug development. *Crit Rev Oncol Hematol* **57:**191–214.

Patrawala L, Calhoun T, Schneider-Broussard R, Li H, Bhatia B, Tang S, Reilly JG, Chandra D, Zhou J, Claypool K, et al. (2006) Highly purified $CD44^+$ prostate cancer cells from xenograft human tumors are enriched in tumorigenic and metastatic progenitor cells. *Oncogene* **25:**1696–1708.

Petrylak DP, Tangen CM, Hussain MH, Lara PN Jr, Jones JA, Taplin ME, Burch PA, Berry D, Moinpour C, Kohli M, et al. (2004) Docetaxel and estramustine compared with mitoxantrone and prednisone for advanced refractory prostate cancer. *N Engl J Med* **351:**1513–1520.

Phatak P, Dai F, Butler M, Nandakumar MP, Gutierrez PL, Edelman MJ, Hendriks H, and Burger AM (2008) KML001 cytotoxic activity is associated with its binding to telomeric sequences and telomere erosion in prostate cancer cells. *Clin Cancer Res* **14:**4593–4602.

Powell BL, Moser B, Stock W, Gallagher RE, Willman CL, Stone RM, Rowe JM, Coutre S, Feusner JH, Gregory J, et al. (2010) Arsenic trioxide improves event-free and overall survival for adults with acute promyelocytic leukemia: North American Leukemia Intergroup Study C9710. *Blood* **116:**3751–3757.

Reya T, Morrison SJ, Clarke MF, and Weissman IL (2001) Stem cells, cancer, and cancer stem cells. *Nature* **414:**105–111.

Shen Y, Shen ZX, Yan H, Chen J, Zeng XY, Li JM, Li XS, Wu W, Xiong SM, Zhao WL, et al. (2001) Studies on the clinical efficacy and pharmacokinetics of low-dose arsenic trioxide in the treatment of relapsed acute promyelocytic leukemia: a comparison with conventional dosage. *Leukemia* **15:**735–741.

Smith V, Dai F, Spitz M, Peters GJ, Fiebig HH, Hussain A, and Burger AM (2009) Telomerase activity and telomere length in human tumor cells with acquired resistance to anticancer agents. *J Chemother* **21:**542–549.

Soignet SL, Frankel SR, Douer D, Tallman MS, Kantarjian H, Calleja E, Stone RM, Kalaycio M, Scheinberg DA, Steinherz P, et al. (2001) United States multicenter study of arsenic trioxide in relapsed acute promyelocytic leukemia. *J Clin Oncol* **19:**3852–3860.

Soignet SL, Maslak P, Wang ZG, Jhanwar S, Calleja E, Dardashti LJ, Corso D, DeBlasio A, Gabrilove J, Scheinberg DA, et al. (1998) Complete remission after treatment of acute promyelocytic leukemia with arsenic trioxide. *N Engl J Med* **339:**1341–1348.

Stuelten CH, Mertins SD, Busch JI, Gowens M, Scudiero DA, Burkett MW, Hite KM, Alley M, Hollingshead M, Shoemaker RH, et al. (2010) Complex display of putative tumor stem cell markers in the NCI60 tumor cell line panel. *Stem Cells* **28:**649–660.

Tang Y, Khan MA, Goloubeva O, Lee DI, Jelovac D, Brodie AM, and Hussain A (2006) Docetaxel followed by castration improves outcomes in LNCaP prostate cancer-bearing severe combined immunodeficient mice. *Clin Cancer Res* **12:**169–174.

Tannock IF, de Wit R, Berry WR, Horti J, Pluzanska A, Chi KN, Oudard S, Théodore C, James ND, Turesson I, et al. (2004) Docetaxel plus prednisone or mitoxantrone plus prednisone for advanced prostate cancer. *N Engl J Med* **351:**1502–1512.

Tsuruo T, Iida H, Tsukagoshi S, and Sakurai Y (1981) Overcoming of vincristine resistance in P388 leukemia in vivo and in vitro through enhanced cytotoxicity of vincristine and vinblastine by verapamil. *Cancer Res* **41:**1967–1972.

Visvader JE and Lindeman GJ (2008) Cancer stem cells in solid tumours: accumulating evidence and unresolved questions. *Nat Rev Cancer* **8:**755–768.

Zhu ML, Horbinski CM, Garzotto M, Qian DZ, Beer TM, and Kyprianou N (2010) Tubulin-targeting chemotherapy impairs androgen receptor activity in prostate cancer. *Cancer Res* **70:**7992–8002.

Address correspondence to: Dr. Arif Hussain, University of Maryland Greenebaum Cancer Center, 22 S. Greene St., Baltimore, MD 21201. E-mail: ahussain@som.umaryland.edu